Supplementary Material (ESI) for Chemical Communications

Biomimetic Design and Assembly of Organic-Inorganic Composite Films with Simultaneously Enhanced Strength and Toughness

Jingbin Han,[a] Yibo Dou,[a] Dongpeng Yan,[a] Jing Ma,[b] Min Wei,[a,]* David G. Evans[a] and Xue Duan[a]

[a] *State Key Laboratory of Chemical Resource Engineering, Beijing University of Chemical Technology, Beijing 100029, P. R. China, Phone: +86-10-64412131. Fax: +86-10-64425385. E-mail: weimin@mail.buct.edu.cn.*

[b] *Mesoscopic Chemistry of MOE, Nanjing University, Nanjing 210093, P. R. China.*

1. Experimental and Computational details

Preparation of Colloidal LDH Suspension: Colloidal LDH nanoplateletes suspension was prepared similar with our previous report[1] by using a method involving separate nucleation and aging steps. Typically, 100 ml of solution A ($Mg(NO_3)_2{\cdot}6H_2O$: 0.2 M and $Al(NO_3)_3{\cdot}9H_2O$: 0.1 M) and 400 ml of solution B (NaOH: 0.15M) were simultaneously added to a colloid mill with rotor speed of 3000 rpm and mixed for 1 min. The resulting LDH slurry was obtained *via* centrifugation and washed twice with deionized water and then dispersed in 400 mL of deionized water. This aqueous suspension was transferred into a stainless steel autoclave with a Teflon lining. After hydrothermal treatment at 110 °C for 24 h, a colloidal suspension containing LDH nanoplatelets with narrow size distribution and aspect ratio of 16–22 was obtained. The concentration of LDH nanoplatelets used for fabrication of hybrid films were 0.1 %, 0.25 % and 0.45 % (wt.%), respectively.

Film Fabrication: Multilayer films of LDH nanoplatelets/PVA were fabricated by applying the

layer-by-layer (LBL) assembly procedure. Quartz glass slides were pretreated in a bath of methanol/HCl (1/1, v/v) and then concentrated H_2SO_4 for 30 min each to make the substrates surface hydrophilic and negatively charged. The deposition procedure was performed with a robotic manipulator (DR-3, R&K Technologies, Germany) programmed to carry out all the operations automatically for n = 1–300. The overall LBL process consists of a cyclic repetition of the following steps: (a) dipping the pretreated substrates into the colloidal LDH suspension containing MgAl-LDH nanoplatelets for 10 min, followed by rinsing with deionized water thoroughly; (b) immersing into an aqueous solution of PVA (MW ≈ 77000, 1 wt.%) for 10 min and washed with deionized water. Subsequently, a series of these operations for LDH nanoplatelets and PVA were repeated n times to obtain $(LDH/PVA)_n$ multilayer films. The resulting films were finally rinsed with deionized water and dried at ambient temperature. The free-standing films were released from the substrates by immersion into 0.2 wt.% aqueous hydrofluoric acid (pH adjusted to 5.5 with NaOH solution) for 30 min. The obtained films were picked up with a 60 meshed sieve and were finally dried in vacuum at room temperature. Glutaraldehyde (GA) cross-linked samples were prepared by immersion of the free-standing films in a GA solution (5 vol.%) for 30 min. The weight fraction of LDH in the LDH/PVA nanocomposite films was controlled by changing the clay concentration in the LBL deposition process.

Sample Characterization: XRD patterns of $(LDH/PVA)_n$ film were performed using a Shimadzu XRD-6000 diffractometer under the following conditions: 40 kV, 30 mA, Cu Kα radiation. The SEM images were obtained on a Zeiss Supra 55 field emission scanning electron microscope. UV-vis absorption spectra were recorded on a Shimadzu UV-2501PC spectrometer. X-ray photoelectron spectroscopy (XPS) measurements were performed using an ESCALAB 250

instrument (Thermo Electron) with Al Kα radiation. TEM image was obtained on JEOL 2010 microscope operating at 200 kV. Loading of LDH in the free-standing film was measured by inductively coupled plasma (ICP) emission spectroscopy (Shimadzu ICPS-7500) by dissolving the samples in dilute HCl. Thermo-gravimetric analyzer (TGA) were carried out on a PCT-1A thermal analysis system under ambient atmosphere with a heating rate of 10 °C/ min. The particle size distribution was determined using a Malvern Mastersizer 2000 laser particle size analyzer. The Fourier transform infrared (FTIR) spectra were obtained using a Vector 22 (Bruker) spectrophotometer with 2 cm^{-1} resolution. The mechanical properties of free-standing hybrid films were measured under tensile mode in a universal mechanical testing machine (Instron, FastTrack 8800 Servohydraulic Systems) with load speed of 0.5 mm/min. Free-standing specimens were obtained by cutting the film into 4 mm wide and 20 mm long stripes. Reported data on elastic modulus, tensile strength and strain at rupture are average of five different stripes of the same sample.

Theoretical Calculation Details: An ideal LDH-NO_3^- double layer model with 6×3×1 supercell of the *R*-3*m* space group was constructed according to our previous work,[2] taking into account the reduction of computational complexity without affecting the precision. As shown in Scheme S1, the supercell containing 24 Mg atoms and 12 Al atoms was built based on the following rule: each [AlO_6] octahedron is surrounded by six [MgO_6] octahedra, and each [MgO_6] octahedron is, in turn, surrounded by three [AlO_6] octahedra, ensuring that Al atoms will not occupy adjacent octahedra. 12 nitrate anions were introduced into the simulated supercell randomly based on the assumption that these anions occupy the whole available interlayer space as much as possible. Subsequently, a bigger supercell with the LDH-NO_3^-

supercell at the centra position was constructed, with lattice parameters a = 18.30 Å, b = 9.15 Å, c = 90 Å (experimental result), $\alpha = \beta = 90$, $\gamma = 120°$. The supercell was treated as P1 symmetry and all the lattice parameters were considered as independent variables in the simulation. A 3-dimensional periodic boundary condition was applied in the system, and the simulated supercell can be repeated infinitely in three directions. 12 PVA with 10 repeated C_2H_4O units were introduced into the simulated supercell with 6 PVA molecules up and down the LDH layer respectively. As a result, the formula of the simulated structure can be expressed as: $Mg_{24}Al_{12}(OH)_{72}(NO_3)_{12}(C_{20}H_{42}O_{10})_{10}$. For the pristine PVA structure as a comparison sample, the LDH-NO_3^- supercell was replaced by two PVA molecules with 10 C_2H_4O repeated units.

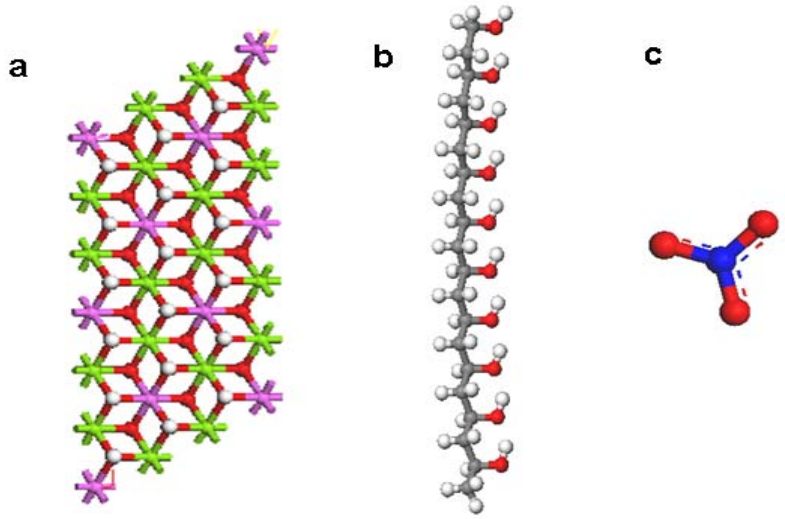

Scheme S1. (a) The 6×3×1 model for the Mg-Al-LDH superlattice layer (white: H; red: O; pink: Al; green: Mg); (b) Structural model of PVA and (c) Structural model of nitrate anion.

A modified cff91 force field was employed to perform MD simulations in the whole process. Charge Equilibration (QEq) method[3] was used to calculate atomic charges of the layer, in which the partial charges are +0.703e for Mg, +1.363e for Al, –0.537e for O and +0.243e for H. The partial charges for nitrate derived from Li's work.[4] Other forcefield

parameters for the anions and water molecules were referred to the cff91 forcefield.[5] The QEq method was also employed to calculate the partial charges of PVA. In potential energy calculations, the long range coulomb interactions between partial charges were computed by the Ewald summation technique[6] and a "spline cutoff" method was used to calculate van der Waals interaction. After energy minimization was applied on the initial model, MD simulations were performed in isothermal-isobaric (NPT) ensemble with the temperature of 300 K and the pressure of 0.1 MPa (about 1 atm). The Andersen method[7] and Berendsen method[8] were used to control temperature and pressure, respectively. The total simulation time was 100 ps with the simulation time step of 1 fs. The result showed that the system reached equilibrium with lattice parameters and total potential energy fluctuating around a constant value within the first 20 ps, so the dynamic trajectories were recorded every 50 fs in the remaining 80 ps in order to analyze the ensemble average values. All the simulations were performed using Discover module in Material Studio software package.[9]

2. Results and Discussion

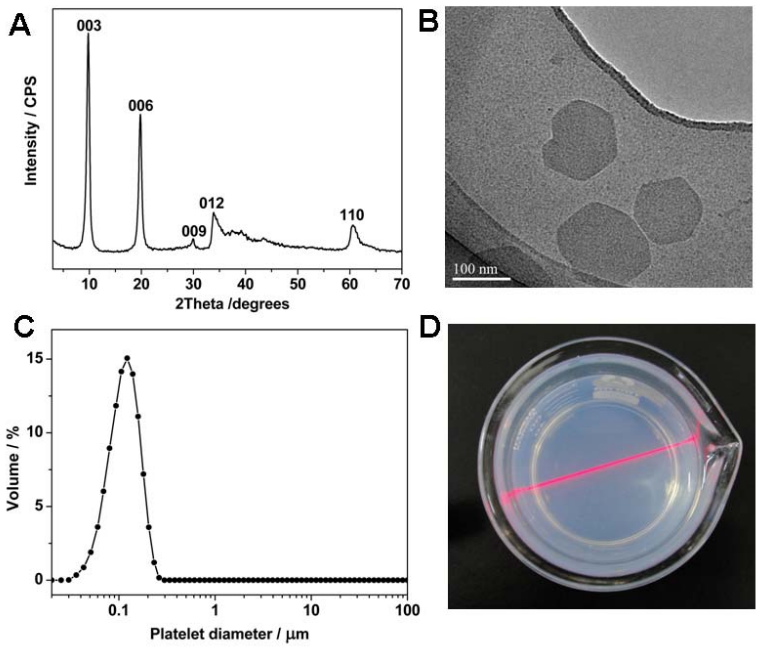

Figure S1 (A) Powder XRD pattern, (B) TEM image, (C) particle size distribution of the MgAl-NO_3 LDH and (D) Digital photograph of its colloidal suspension.

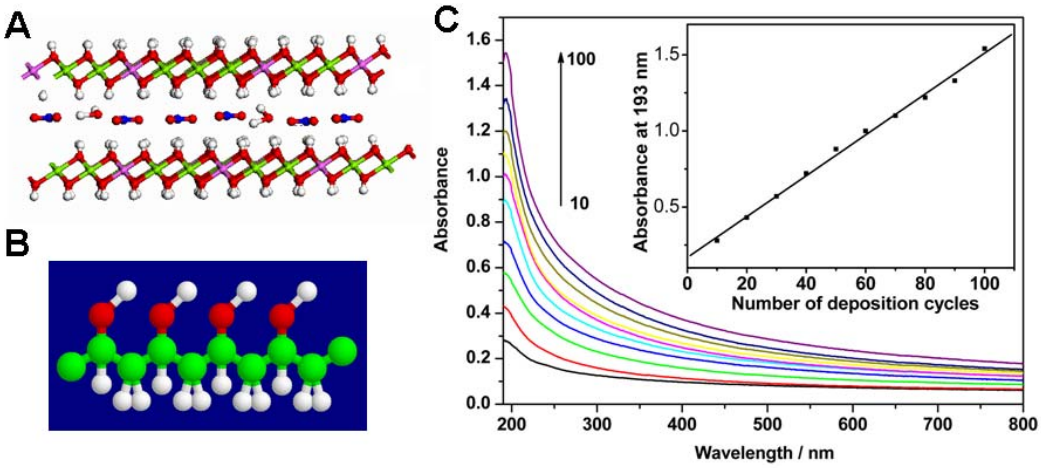

Figure S2 (A) General crystal structure of LDH (pink, Mg; green, Al; red, O; white, H; blue, N); (B) Molecular structure of PVA (green, C; red, O; white, H); (C) UV-vis absorption spectra of the $(LDH/PVA)_n$ (n = 10–100) films assembled on quartz glass slides. The absorbance at 193 nm is plotted against the bilayer number in the inset.

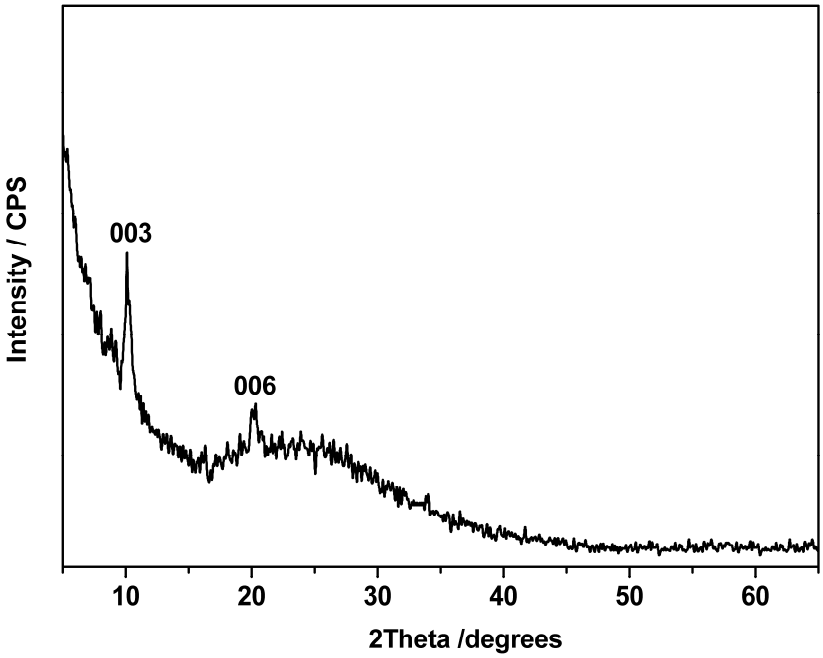

Figure S3. XRD pattern of the $(LDH/PVA)_{300}$ nanocomposite film.

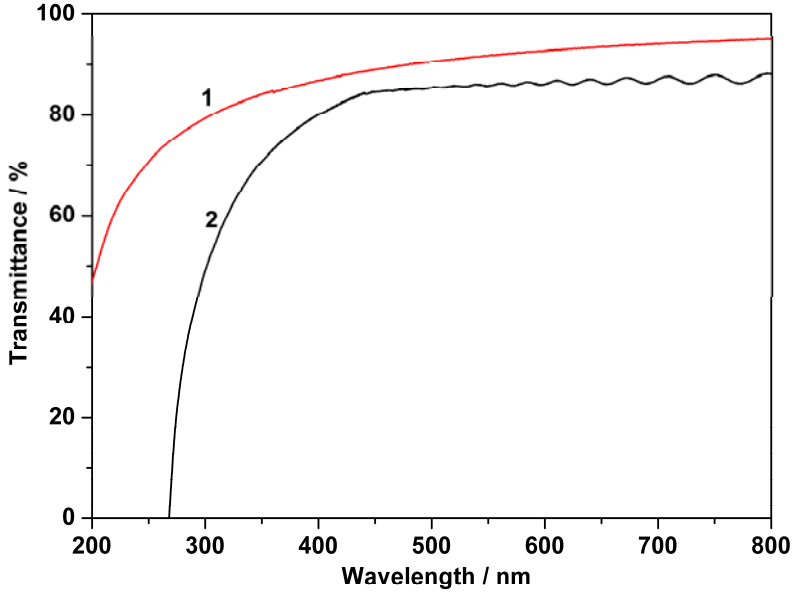

Figure S4 UV-Vis transmittance spectra of (1) pure PVA cast film and (2) the $(LDH/PVA)_{300}$ nanocomposite film.

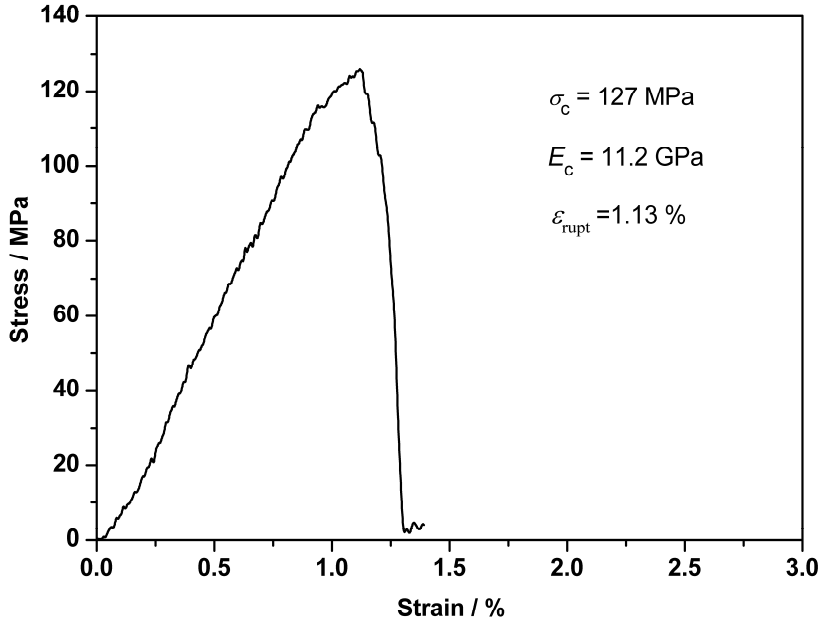

Figure S5 Stress–strain curve of the $(LDH\text{-}NS/PVA)_{300}$ film using exfoliated LDH nanosheets with aspect ratio of 500–5000 as building blocks.

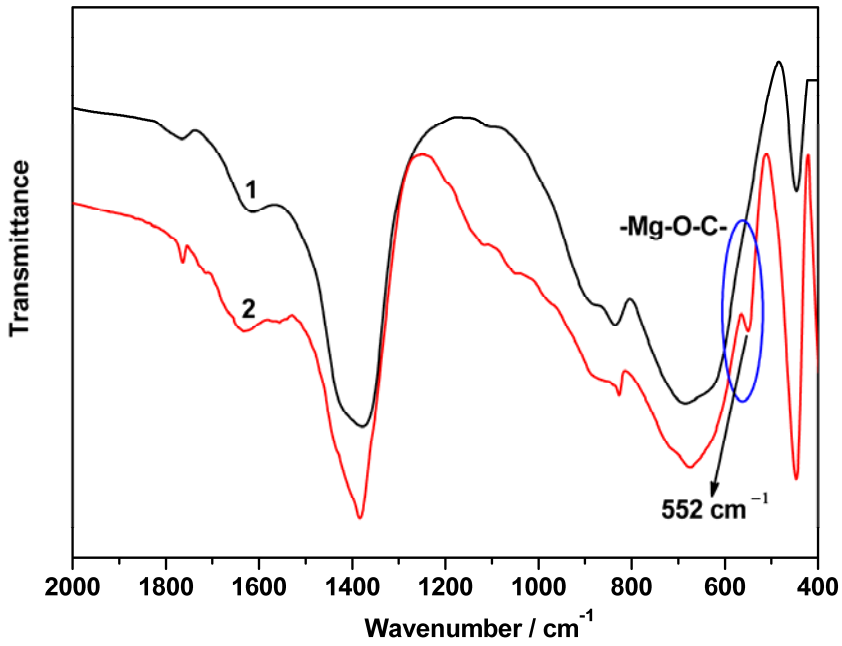

Figure S6 FTIR spectra of (1) LDH and (2) LDH after treatment by GA. The appearance of the peak at 552 cm^{-1} in the red curve is associated with the formation of –Mg–O–C– bond.

GA is a highly efficient cross-linking agent for PVA that forms covalent acetal bridges between –OH groups of the polymer chains.[10] The availability of GA to cross-link LDH platelets was confirmed by FTIR spectra (Figure S6). An absorption band at 552 cm^{-1} corresponding to

stretching vibration of –Mg–C–O– appeared for the LDH-GA composite compared with that of pure LDH, confirming the cross-linking of hydroxyl groups on the surface of LDH nanoplatelets by GA.

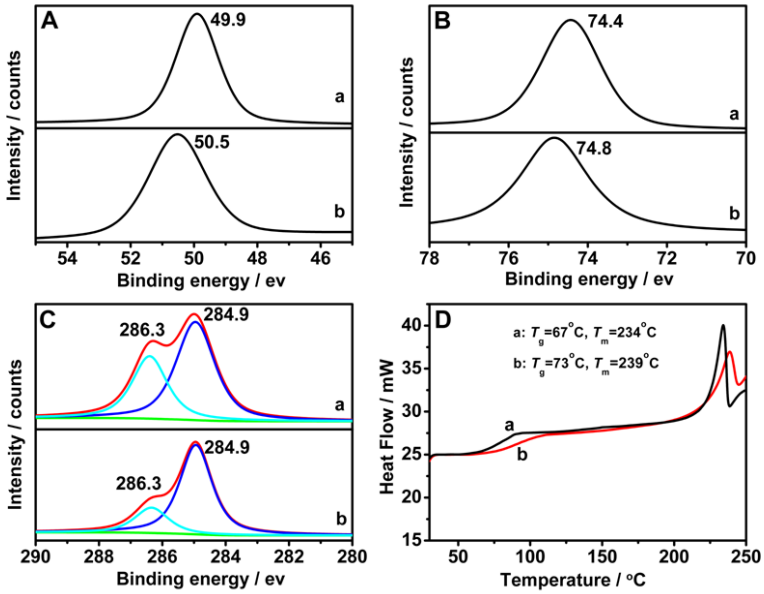

Figure S7 (A) Mg and (B) Al 2p orbital XPS spectra for (a) LDH and (b) LDH/PVA nanocomposite; (C) C 1s orbital XPS spectra for (a) PVA and (b) LDH/PVA nanocomposite; (D) DSC results for (a) PVA and (b) LDH/PVA nanocomposite.

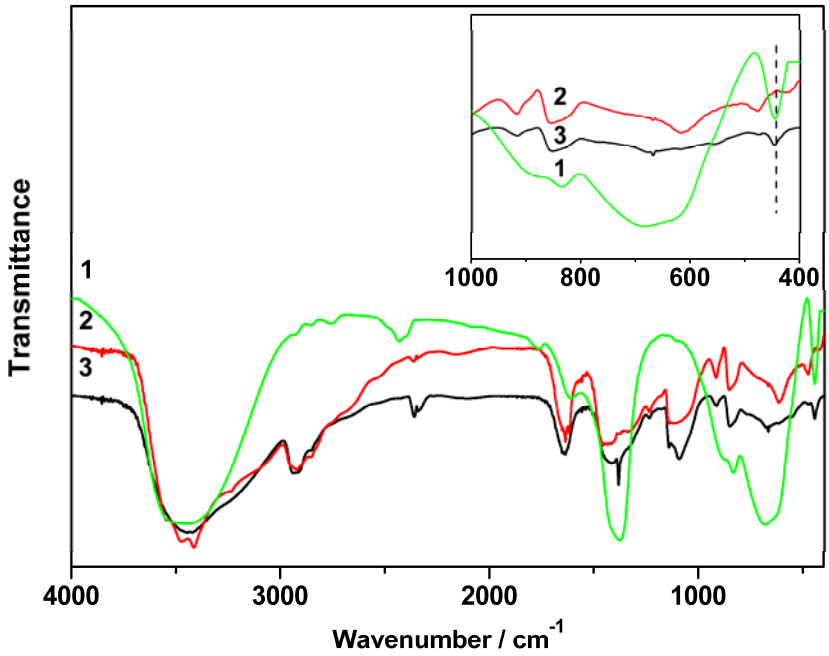

Figure S8 FTIR spectra for (1) LDH, (2) PVA and (3) LDH/PVA nanocomposite; inset: close-up of the peaks below 1000 cm^{-1}.

The formation of Al–PVA and Mg–PVA bonds can be further verified by the strong suppression of the lattice vibration at 450 cm^{-1} and translational vibration of hydroxyl between 500 and 1000 cm^{-1} in the LDH nanoplateletes from FTIR spectra (Figure S8).

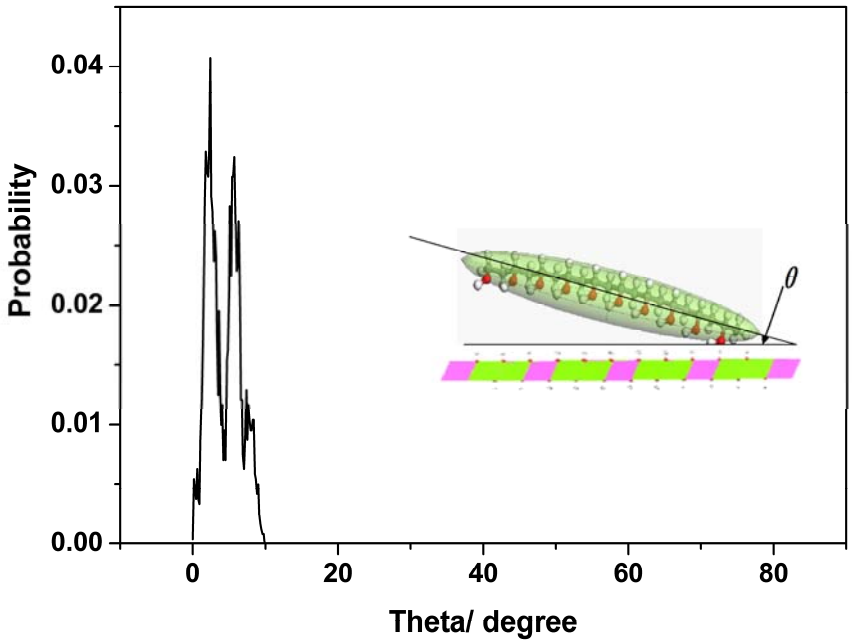

Figure S9 The orientation angel (θ) distribution for the LDH/PVA system; θ was defined as the angle of the line connecting the terminal carbon atoms of PVA relative to the LDH layer (shown in the inset).

To better understand the geometric structure, supermolecular interactions and mechanical properties of the LDH/PVA nanocomposite system, classical molecular dynamic simulations were performed for the idealized models of both the LDH/PVA and the pristine PVA structure. The organic PVA molecules were found to adopt an ordered arrangement with a preferred orientation in the as-prepared LDH/PVA film. This ordered arrangement originated from the hydrogen bond between the –OH group in PVA and those in the LDH layer. Additionally, the distance between the terminal carbon atoms in PVA decreased by ca. 5% compared with that in the fully extended form, suggesting that the PVA molecules are flexible enough upon interacting with the LDH platelets.

References:

[1] (a) J. Han, Y. Dou, M. Wei, D. G. Evans and X. Duan, *Angew. Chem. Int. Ed.*, 2010, **49**, 2171; (b) Y. Zhao, F. Li, R. Zhang, D. G. Evans and X. Duan, *Chem. Mater*., 2002, **14**, 4286.

[2] (a) D. P. Yan, J. Lu, J. Ma, M. Wei, S. Qin, L. Chen, D. G. Evans and X. Duan, *J. Mater. Chem.*, 2010, **20**, 5016; (b) D. P. Yan, J. Lu, L. Chen, S. Qin, J. Ma, M. Wei, D. G. Evans and X. Duan, *Chem. Commun.*, 2010, **46**, 5912.

[3] A. K. Rappé and W. A. Goddard, *J. Phys. Chem*., 1991, **95**, 3358.

[4] H. Li, J. Ma, D. G. Evans, T. Zhou, F. Li and X. Duan, *Chem. Mater.*, 2006, **18**, 4405.

[5] (a) J. R. Maple, M.-J. Hwang, T. P. Stockfisch, U. Dinur, M. Waldman, C. S. Ewig and A. T. Hagler, *J. Comput. Chem.*, 1994, **15**, 162; (b) D. P. Yan, J. Lu, M. Wei, H. Li, J. Ma, F. Li, D. G. Evans and X. Duan, *J. Phys. Chem. A*, 2008, **112**, 7671; (c) D. P. Yan, J. Lu, M. Wei, J. Ma, D. G. Evans and X. Duan, *Phys. Chem. Chem. Phys.*, 2009, **11**, 9200.

[6] (a) M. P. Allen and D. J. Tildesley, *Computer Simulation of Liquids*, Clarendon, Oxford, 1987; (b) A. R. Leach, *Molecular Modeling, Principles and Applications*, Pearson Education Ltd, England, 2nd edn. 2001.

[7] H. C. Andersen, *J. Chem. Phys*., 1980, **72**, 2384.

[8] H. J. C. Berendsen, J. P. M. Postma, A. van Gunsteren, A. DiNola and J. R. Haak, *J. Chem. Phys.*, 1984, **81**, 3684.

[9] *Discover Module, MS Modeling*, Version *2.2*; Accelrys Inc.: San, Diego, CA, 2003.

[10] C. Tang, C. D. Saquing, J. R. Harding, S. A. Khan, *Macromolecules*, 2010, **43**, 630.